Aluminum Alloys Anodisation for Nanotemplates Application

N. Tsyntsaru[a,b]

[a]*Institute of Applied Physics of the ASM,*
5, Academiei, str., Chisinau, MD-2028, Republic of Moldova, e-mail: ashra_nt@yahoo.com
[b]*Vilnius University,*
24, Naugarduko, str., Vilnius, LT-03325, Lithuania

The aim of this investigation was to reveal the processing differences in achieving nanoporous anodized aluminium from aluminium alloys and their application for cobalt nanowires electrodeposition. The following types of aluminium were tested: pure Al (99.99%), commercial AA1050 alloy, commercial 6082 alloy and commercial 6060 alloy. Because of the differences in the surface temperature and high voltages during the anodizing steps, some stresses can be built up in the material. Therefore a strict temperature control should be was done to limit thermal stresses in materials. Alloying elements (Si, Mg) cause precipitates that are observed on the surface, especially for 6060 alloy. Nevertheless, a nanoporous structure can be obtained at the end of second anodization step on all aluminium alloys investigated. It was shown that the number density of pores on the surface is practically independent on the aluminium alloys used. However, the degree of hexagonal distribution of the pores depends on the type of anodized aluminium alloy. Also, a successful fabrication of Co nanowire arrays using nanoporous anodic alumina template produced on Al alloy has been demonstrated, and the uniform filling of the template by cobalt nanowires arrays is discussed.

Keywords: commercial aluminium alloys, nanoporous anodic alumina template, cobalt nanowires, uniform filling.

УДК 544.653.2

The anodization of aluminium is an electrochemical process resulting in surface passivation and obtaining of distributed pores on the surface. In 1995 Masuda et al. reported a two-step anodization which leads to a regular distribution of the pores due to a self-organization process [1]. Anodic aluminium oxide (AAO) is very important material in nanotechnology applications. It is basically used as a template for production of nanorods, nanowires and nanotubes. Easy and low costly control of properties such as pore diameter, interpore distance, tube height, time and temperature are advantages of AAO in nanotechnologies since controlling these also means controlling properties of nanostructured materials. This raises an increasing interest in these pores as they offer structures in the nanometer scale which can be used in various applications such as magnetic storage [2], solar cells [3], carbon nanotubes [4], catalysts [5] and metal nanowires [6], as well as the substrates for artificial lipid membranes [7]. Besides production of nanostructured materials, nanoporous AAO is an option for applications where self-lubricating might be needed [8–11]. A high purity aluminum foil (min 99.99% of Al) is usually used mostly as a substrate for anodization in order to produce ordered nanoporous templates [1, 12, 13].

However, during anodization electrolyte can affect the composition of the oxide film and contaminate it. Anodic aluminium oxides have an outer oxide that starts at oxide-electrolyte interface and an inner oxide which starts at oxide-metal interface. Outer oxide consists of alumina containing incorporated anions while inner oxide actually consists on high purity amorphous alumina [9]. These incorporated anions should be taken into account when final AAO is used in different applications.

The aluminium alloys, from the economical point of view, are very interesting materials because of their reasonable price – a thousand times cheaper than high purity aluminium. Another issue is that the alloys give possibilities for specific use depending on alloying elements. There are only few reports subjected on the alloys anodizing [8, 14, 15]. Synthesis of AAO template from the alloys is complicated issue and often requires the specific conditions [15], outstanding from those usually applied to a pure aluminum anodization.

The main aim of this work was to find out if there is any correlation between alloy used for anodization and structural features, and nanopore arrangement of anodic alumina layers formed by two-step anodizing of low purity aluminum in the sulphuric acid electrolyte. The following types of aluminium were tested: pure Al (99.99%), commercial AA1050 alloy, commercial 6082 alloy and commercial 6060 alloy. Each step of nanoporous oxide formation

Table 1. Composition limits (wt.%) of the tested aluminium alloys

Metals present in alloys	AA1050 alloy	6082 alloy	6060 alloy
	wt.%		
Si	0.25	0.7–1.3	0.30–0.6
Fe	0.40	0.5	0.10–0.30
Cu	0.05	0.10	0.10
Mn	0.05	0.40–1.0	0.10
Mg	0.05	0.60–1.2	0.35–0.6
Cr	–	0.25	0.05
Zn	0.07	0.20	0.15
Ti	0.05	0.10	0.10
Others (total)	0.03	0.15	0.15
Al	Min. 99.5	Balance	Balance

(from Al electropolishing to second anodizing) is discussed in details. Moreover, the fabrication of Co nanowire arrays using nanoporous anodic alumina template produced on Al alloys has been carried out.

EXPERIMENTAL PROCEDURE

As aaterial, the following types of aluminium were anodized under the same operating conditions: pure Al (99.99%), commercial AA1050, 6082 and 6060 alloys (Table 1).

Cleaning and Electropolishing

Prior to any anodizing of industrial aluminium sheets, the samples have been ultrasonically degreased in acetone and ethanol followed by a rinsing with deionised water. Dependent on the type of oil or grease contamination present on industrial samples, the thoroughly cleaning may require a more drastic cleaning process. In order to achieve a good nanoporous anodization, an electropolishing of the samples has to be performed before starting up the anodizing process itself. In that respect, pure aluminium and Al alloys were electropolished at a constant current density of 500 $mA \cdot cm^{-1}$ for 1 min. The electrolyte used contain $HClO_4$ (60 wt%) and C_2H_5OH (abs.) in a volumetric ratio of 1:4. The bath temperature was kept low by preference at about ~ 7–10°C. It should be mentioned that electropolishing reaction is not accompanied by oxide formation. Surface smoothing efficiency is limited to coarser textures on the surface [16–19].

First anodization

Anodizing of electropolished samples was carried out in a sulphuric bath to produce nanoporous anodised aluminium surfaces. The first anodizing was performed in a 20 wt% sulphuric acid electrolyte using a two electrode electrochemical cell set up with a magnetic stirrer rotating at 500 rpm. The temperature was kept at ~ 0–1°C during anodizing at a potential of 21 V for 10 min.

Oxide removal

After the first anodizing step, samples have been rinsed with deionised water and then immersed in a solution of CrO_3 (1.8 wt%) and H_3PO_4 (6 wt%) for 30 min at ~ 60°C to achieve a removal of oxide layer obtained during the first anodizing. In that way, a pre-patterning of the aluminium surface is obtained allowing the growth of a more or less regular hexagonal pattern of nanopores to grow during the second anodization. Depending on the type of aluminium alloy used, the duration of the oxide removal step has to be experimentally selected. It is important to avoid a complete removal of the first anodizing layer since that will hinder the regular growth of a nanopattern of pores during the second anodization.

Second anodization

This second anodization was performed under similar conditions as the first anodising, namely in a sulphuric bath at a constant potential of 21 V for 15 min at ~ 1°C. The expected thickness of the anodized layer is ~ 10 μm with a pore diameter of about ~ 20–25 nm.

It should be mentioned that in the case of aluminium alloys treatment and/or on anodizing thick samples one has to be aware of a possible risk of heating up of the samples due to high currents (voltages) applied during electropolishing. This seems to be even more critical in the case of highly alloyed aluminium. After each anodisation step (including electropolishing and oxide removal), SEM images have been taken in order to evaluate the influence of the condition on the each anodising step and after electropolishing.

Cobalt electrodeposition

Following the second anodization, the voltage was systematically reduced to promote thinning of the barrier layer that formed between the porous alumina and the Al substrate, thus facilitating the

electrodeposition of metal. Barrier layer thinning was conducted by reducing the voltage by 2 $V \cdot min^{-1}$ to 15 V, 1 $V \cdot min^{-1}$ to 10 V. The anodization was then continued for 5 min at this final voltage to equilibrate the barrier layer. The cobalt nanowires were electrodeposited from the electrolyte consisting of 100 $g \cdot l^{-1}$, $CoSO_4$ and of 30 $g \cdot l^{-1}$ boric acid under alternative current (AC) and pulse current (PC). The pH value of the electrolyte solution was about 4. The AC electrodeposition was carried out using a 200 Hz sine waveform (reductive time = oxidative time = 2.5 ms) in which the deposition voltage was 30 $V_{pick–pick}$ (where reductive and oxidative voltages are –15 V and 15 V, respectively). The pulse electrodeposition was carried out with different reductive/oxidative conditions using sine waveform also. The deposition parameters were selected as $t_{reductive}$ = $t_{oxidative}$ = 2.5 ms and t_{off} = 30 ms, and 70 ms. Scanning electron microscopy was used to confirm the morphology of the samples. Also focus ion beam (FIB) where used to evaluate the uniformity of grow of Co nanowires along the AAO template.

RESULTS AND DISCUSSION

Anodisation of Aluminium alloys

During anodization of aluminium, oxygen evolves and covers the anode and AAO is formed. Anodizing occurs on the interchange surface between aluminium and aluminium oxide which grows inwards aluminium. Under applied potential, electric field focuses on fluctuations locally, leading to temperature or/and field-enhanced dissolution of the oxide via the shortest paths between the base metal and the electrolyte. As dissolution carries on until the bottoms of the tubes reach the same level and current density decreases. Once each tube has the same height current density becomes steady. Ions move by high field conduction via this path. Oxygen containing ions O^{-2}/OH^{-} immigrate to the bottom of the pore from the electrolyte and reacting with aluminium, they form Al_2O_3 at metal-oxide interface as in barrier type oxides. Meanwhile, at oxide-electrolyte interface at the bottom of the tubes, alumina dissolves. Pores grow inwards aluminium according to this mechanism. The part of the barrier oxide formed at the early stage of pore formation becomes a part of the cell wall while the bottom goes deep inside making the tubes thicker. Pore diameter remains fixed.

The thickness of the barrier film is also constant during this process due to formation and dissolution reactions occurring simultaneously. This lets the potential applied and the current remain stable while the film thickness [9, 12]. The spontaneous reaction causing the formation of aluminium oxide in air atmosphere can be linked to the large negative Gibb's free energy changes. The driving force behind the self-assembly of AAO is linked to the repulsive forces between adjacent pores causing mechanical stress. These repulsive forces are occurring because of the density difference between aluminium and alumina. Atomic density of aluminium in Al_2O_3, is lower than that in the metallic aluminium by a factor of 2, therefore the volume of anodized alumina expands to approximately twice regarding the original volume. This volume expansion leads to a compressive stress at oxide-metal interface pushing the pore walls vertically. If the stress is too high, no pores are generated. Disordered structure is obtained if the stress is too small. In case of moderate forces, pores grow in an ordered manner [12].

The fabrication of alumina templates using pure and commercial aluminum alloys yields the different morphology of the samples at each step of the process (Table 2). The thickness of the obtained anodized layer was ~ 10 μm with a pore diameter of about ~ 20–25 nm. It seems that the density of pores on the surface is almost independent on the type of aluminium alloys used. On the contrary, the degree of hexagonal distribution of the pores depends on the type of anodized aluminium alloy (Table 2). In the first anodization step, porous structure starts to form. However, the arrangement of pores is not really ordered (Table 2). Pores start to grow inwards aluminium base in the random directions until a period when all the tube bottoms are at the same level and parallel to each other. This is a case when oxide removal process is carried out. By removing this oxide, a pre-pattern is produced on aluminium for the second anodization step during which well-ordered structure is obtained (Table 2). Finally, the second anodization, which is basically the same as the first one, is performed to produce a surface consisting of well-ordered nanopores [12, 13, 20, 21].

Because of the differences in the surface temperature and high voltages applying for anodization, some stresses can be built up in the material. Therefore, a strict temperature control should be done to limit thermal stresses in materials (Figure 1). Characterization of the stress state of the materials (cold rolled, annealed, percentage of alloying elements, thickness of the sheets etc.) to be anodized is another parameter that should be taken into consideration. Alloying elements (Si, Mg) seems to be cause precipitates on surface that are seen in the SEM pictures, especially for 6060 alloy (Table 2, white bumps on the surface after second anodization). Nevertheless, a nanoporous structure can be obtained at the end of second anodization step on all investigated aluminium alloys.

Table 2. SEM images of the surfaces of pure Al and Al alloys at all stages of the template synthesis.

99,99 Al	AA1050 Alloy	6082 Alloy	6060 Alloy
Initial surface			
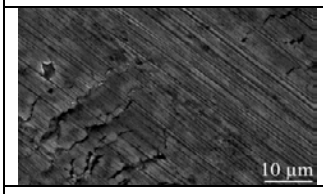	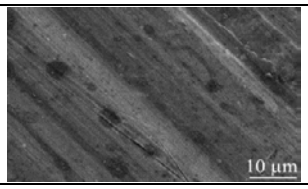		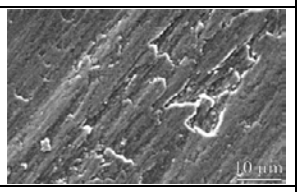
After electropolishing			
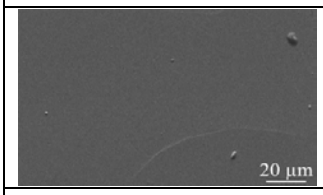	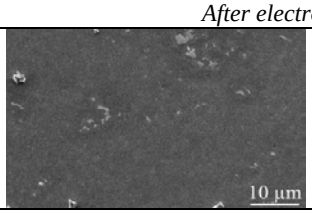	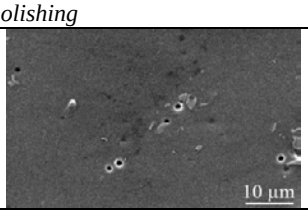	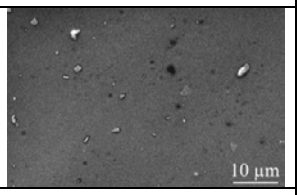
After first anodization			
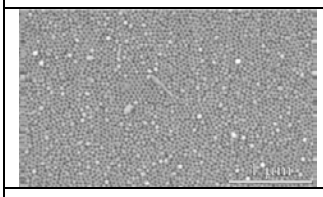	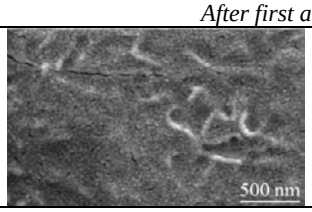	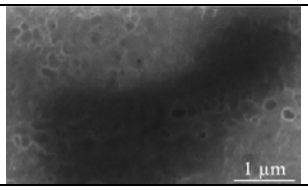	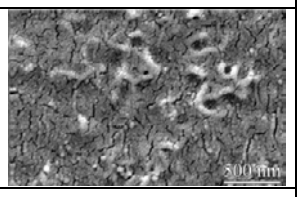
After oxide removal			
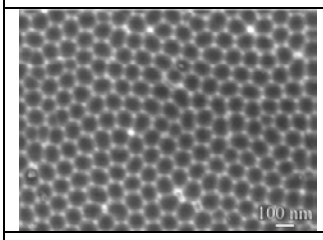	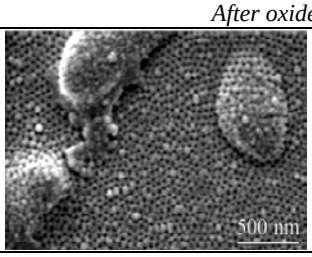	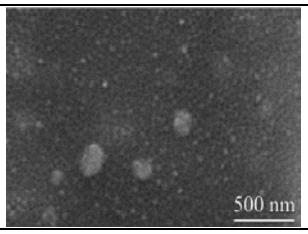	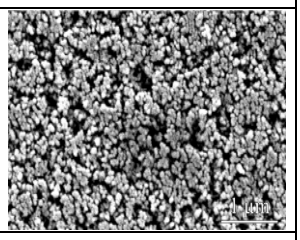
After second anodization			
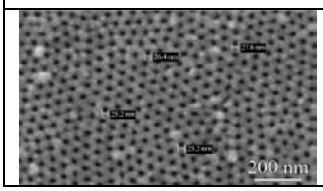	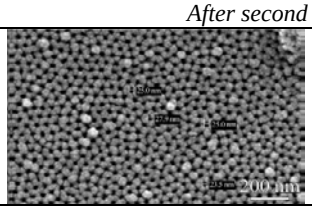	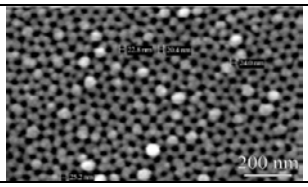	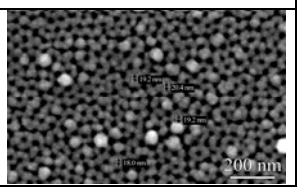

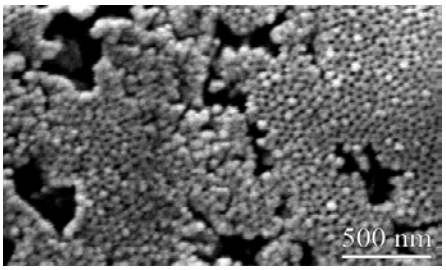

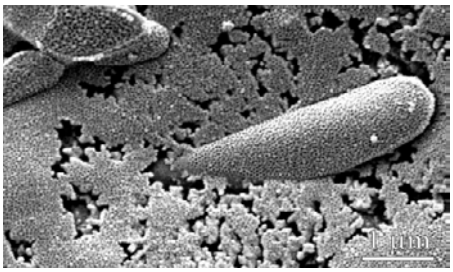

Fig. 1. SEM images of the surfaces of the Al alloys after second anodization, when temperature control failed.

The obtained nanoporous AAO materials can serve as a perfect template for fabrication of nanostructural materials. Electrodeposition is simple and effective for producing high quality nanowires upon the AAO template. Two common electrodeposition methods can be used to obtain uniform and complete filling of the pores of the AAO template. In the first method, a direct current (DC) is used for the deposition. The DC method requires a through-hole AAO template that needs to be detached from the Al substrate. Subsequently, a conductive film must be sputtered on one side of the template before proceeding with deposition. For most nanostructure applications, the thickness of an AAO template is required only a few hundred nanometers. However, for transferring and handling, the thickness of a free-standing AAO template should be thick enough. In the contrast, the AC method and pulsed electrodeposition method allow us directly to deposit metal nanowires into the pores of an AAO template with Al substrate still present.

Several attempts to apply PC mode were made by varying the value of t_{off} to deposit Co into the pores of the alumina. Typical cross section SEM micro-

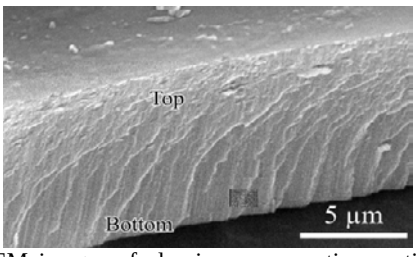

Fig. 2. SEM images of alumina cross section partially filled with Co using AC electrodeposition ($\tau_{ox/red}$ = 2.5 ms, τ_{off} = 30 ms, t = 10 min).

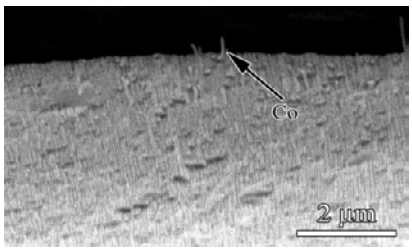

Fig. 3. SEM images of alumina cross section filled with Co using AC electrodeposition (f = 200 Hz, t = 15 min).

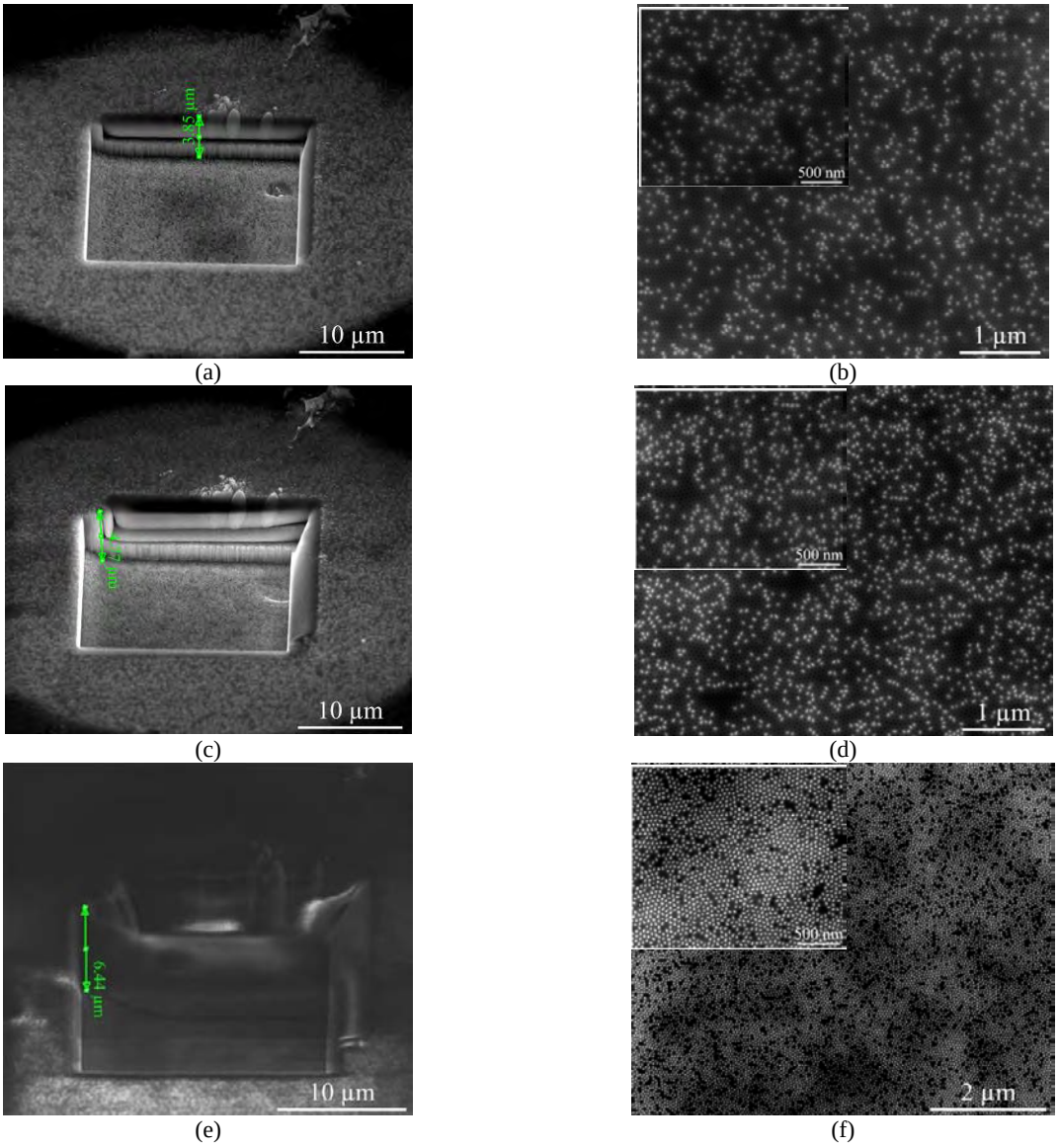

Fig. 4. SEM images of top surfaces of ion-milled Co-filled templates to show degree of pore-filling as a function of depth: (a), (b) 3.85 µm, (c), (d) 4.77 µm and (e), (f) 6.44 µm removed from the top of the 12 µm deep-pores.

graphs of Co nanowires were made using back-scattered electrons mode to maximize atomic number contrast and spectra analysis were carried out. The first successful condition was observed in the case of $t_{reductive}$ = $t_{oxidative}$ = 2.5 ms and t_{off} = 30 ms, but no total pores filling was reached (Fig. 2) only the bottom site of the membrane was filled with Co, that was detecting during EDX analysis.

The AC electrodeposition was carried out using different frequencies (50–1000 Hz) as sine waveform (reductive time = oxidative time = 2.5 ms) in which the deposition voltage was 30 $V_{pick–pick}$. It was revealed that the optimal frequency is closed to 200 Hz (Figure 4). Thus, under these conditions we could reach the growth on the entire length of the AAO template of the cobalt nanowires (Figure 4).

In order to investigate the membrane pores filling by cobalt, a FIB analysis was performed on the most successful samples obtained under optimal electrodeposition conditions: $V_{pick–pick}$ = 30 V, f = 200 Hz, and t = 20 min. The fraction of pores filled as a function of depth beneath the initial electrode surface is presented in the Figure 4. Where the fraction of pores filled is the ratio between white dots (Co nanowires) and dark dots (empty AAO) estima-ted from FIB/SEM pictures.

FIB analysis (Fig. 4) revealed different picture in comparison with data received from SEM images of alumina cross-section (Figure 3). Nevertheless, that cobalt was deposited along entire length of AAO template as it seen from Fig. 3, the true picture of alumina filling by cobalt nanowires vary from those images. Thus, the fraction of pores filled 3.8 μm below the top of AAO surface is ca. 30% only (Fig. 4a,b), by going deeper with ion beam we can found that close to 50% of cobalt nanowires filling can be reached (Fig. 4c,d), while the fraction filled to a level of 6.5 μm below the initial surface is ~ 85% (Fig. 4e,f). The most probable explanation of non-uniform filling of AAO by cobalt nanowires can be given taking into account that side reaction accompanying cobalt electrodeposition is hydrogen evolution, which can block the pores randomly. The hydrogen evolution will influence drastically on the uniformity of nanowires growth, and result is seen in Figure 4. Thus, AC method gives a good possibility to deposit cobalt nanowires into AAO without removing of the barrier layer, but electrodeposition should be performed only for short times (short nanowires will be obtained), because in this case blocking pores by hydrogen is overcoming. In addition, diffusion limits of the Co(II) into pores exist, which is the second major factor affecting the uniformity of grow.

CONCLUSIONS

We demonstrated a successful anodization of industrial aluminum alloys in order to obtain ordered nanoporous structure using the common procedure. The effect of the temperature rising during alloys anodization should be taken into account to avoid failure in receiving ordered pores. Different electrochemical conditions and porous alumina were applied for template synthesis of cobalt nanowire arrays, revealing several cases. It was shown the possibility to deposit Co under AC electrodeposition mode in the produced AAO. The study under different AC conditions current frequencies (50–1000 Hz), V_{p-p} = 30 V, revealed that the optimal frequency is in the range 150–200 Hz. Using pulse AC electrodeposition mode does not improve the uniformity of pores filling.

ACKNOWLEDGMENTS

This research received funding from FP7 Oil&Sugar project (295202). Also, partial funding was granted by the Research Council of Lithuania (MIP-031/2014) and Moldavian national projects (14.02.121A), (14.819.02.16F).

REFERENCES

1. Masuda H., Fukuda K. Ordered Metal Nanohole Arrays Made by a Two-Step Replication of Honeycomb Structures of Anodic Alumina. *Science*. 1995, **268**, 1466–1468.
2. Nielsch K., Wehrspohn R.B., Barthel J., Kirschner J., Gioisele U., Fischer S.F., Kronmuller H. Hexagonally Ordered 100 nm Period Nickel Nanowire Arrays. *Appl Phys Lett*. 2001, **79**(9), 1360–1362.
3. Karmhag R., Tesfamichael T., Wackelgard E., Niklasson G.A., Nygren M. Oxidation Kinetics of Nickel Particles: Comparison between Free Particles and Particles in an Oxide Matrix. *Sol Energy*. 2000, **68**(4), 329–333.
4. Che G., Lakshmi B.B., Fisher E.R., Martin C.R. Carbon Nanotubule Membranes and Possible Applications to Electrochemical Energy Storage and Production. *Nature*. 1998, **393**, 346–347.
5. Che G., Lakshmi B.B., Martin C.R., Fisher E.R., Ruoff R.S. Chemical Vapor Deposition (CVD)-Based Synthesis of Carbon Nanotubes and Nanofibers Using a Template Method. *Chem Mater*. 1998, **10**(1), 260–267.
6. Zhang Z.B., Gekhtmann D., Dresselhaus M.S., Ying J.Y. Processing and Characterization of Single-Crystalline Ultrafine Bismuth Nanowires. *Chem Mater*. 1999, **11**(7), 1659–1665.
7. Hennesthal C., Drexler J., Steinem C. Membrane Suspended Nanocompartments Based on Ordered Pores in Alumina. *Chem Phys Chem*. 2002, **10**, 885–889.
8. Zaraska L., Sulka G.D., and Jaskula M. Porous Anodic Alumina Membranes Formed by Anodization of AA1050 Alloy as Templates for Fabrication of Metallic Nanowire Arrays. *Surf Coat Technol.* 2010, **205**(7), 2432–2437.
9. Hagelsieb L.M. Anodic Aluminum Oxide Processing, Characterization and Application to DNA Hybridization Electrical Detection, *PhD. Thesis*, Universite Catholique de Louvain, Louvain-La-Neuve, Belgique, 2007, 229 p.
10. Özturk S., Taşaltin N., Kilinç N., and Öztürk Z.Z. Fabrication of ZnO Nanotubes using AAO Template and Sol-gel Method. *J of Optoelectronic and Biomedical Materials.* 2009, **1**, 15–19.
11. Skeldon P., Wang H.W., and Thompson G.E. Formation and Characterization of Self-lubricating MoS_2 Precursor Films on Anodized Aluminium. *Wear.* 1997, **206**, 187–196.

12. Choi J. Fabrication of Monodomain Porous Alumina Using Nanoimprint Lithography and Its Applications, *PhD. Thesis*, Martin-Luther-Universitat Halle, Wittenberg, Germany, 2004, 103 p.

13. Lee W. The Anodization of Aluminium for Nanotechnology Applications. *JOM*. 2010, **62**, 57–63.

14. Zaraska L., Sulka G.D., Szeremeta J., Jaskula M. Porous Anodic Alumina Formed by Anodization of Aluminum Alloy (AA1050) and High Purity Aluminum. *Electrochim Acta*. 2010, **55**(14), 4377–4386.

15. Zaraska L., Kurowska E., Senyk I., Jaskula M. The Effect of Anode Surface Area on Nanoporous Oxide Formation during Anodizing of Low Purity Aluminium (AA1050 Alloy). *J Solid State Electrochem*. 2014, **18**, 361–368.

16. Jiang C.X., Tu J.P., Guo S.Y., Fu M.F., and Zhao X.B. Friction Properties of Oil-infiltrated Porous AAO Film on an Aluminium Substrate. *Acta Metall Sin Engl*. 2005, **18,** 249–253.

17. Lillo M., and Losic D. Pore Opening Detection for Controlled Dissolution of Barrier Oxide Layer and Fabrication of Nanoporous Alumina with Through-hole Morphology. *J Membrane Sci*. 2009, **327,** 11–17.

18. Ma D., Li S., and Liang C. Electropolishing of High-purity Aluminium in Perchloric Acid and Ethanol Solutions. *Corros Sci*. 2009, **51,** 713–718.

19. Lee G.S., Choi J.H., Choi Y.C., Bu S.D., and Lee Y.Z. Tribological Effects of Pores on an Anodized Al Alloy Surface as Lubricant Reservoir. *Curr Appl Phys*. 2011, 11, S182–S186.

20. Zhao S., Chan K., Yelon A., and Veres T. Novel Structure of AAO Film Fabricated by Constant Current Anodization. *Adv Mater*. 2007, **19**, 3004–3007.

21. Sulka G.D., and Parkola K.G. Anodizing Potential Influence on Well-ordered Nanostructures Formed by Anodization of Aluminium in Sulphuric Acid. *Thin Solid Films*. 2006, **515**, 338–345.

Received 15.07.15

Реферат

Целью данного исследования было выявить есть ли различия при обработке промышленных алюминиевых сплавов для получения нанопористого анодированного алюминия, и их использование в качестве темплата для электроосаждения нанопроводов кобальта. В данной работе анодировались следующие типы алюминия: Al (99,99%), промышленные сплавы AA1050, 6082 и 6060. Из-за различий в температуре поверхности и высоких потенциалов во время анодирования, остаточные напряжения могут накапливаться в материале, особенно в промышленных сплавах. Поэтому должен проводится строгий контроль температуры, чтобы ограничить термические напряжения в материале. Присутствие легирующих элементов (Si, Mg) приводит к появлению осадков на поверхности, особенно для сплава 6060. Нанопористая структура может быть получена для всех исследованных в данной работе алюминиевых сплавов в результате двухстадийного анодирования. Было установлено, что пористость анодированного сплава в основном не зависит от типа используемых алюминиевых сплавов, в то время как степень гексагонального распределения пор зависит от типа анодированного алюминиевого сплава. Также было показано, что возможно успешное изготовление массивов нанопроводов кобальта с использованием темплата нанопористого анодного оксида алюминия, полученного из сплавов алюминия. Была исследована однородность заполнения темплата массивом из нанопроволок кобальта.

Ключевые слова: промышленные алюминиевые сплавы, темплат нанопористого анодного оксида алюминия, нанопроволки кобальта, однородное заполнение.